

results also suggest that kinetic or structural constraints are imposed on the rotated myosin heads, since the speed of actin filaments sliding away from the center of the myosin filament is about nine times less than that of actin filaments sliding toward the center of the myosin filament. The rotated myosin heads may be constrained so that the detachment of the rotated myosin heads from actin would occur at a much slower rate than that which normally occurs. Alternatively, the distance of the power stroke of the rotated head may be less than if the head is not rotated.

In the *in vitro* motility assay the rate of translocation of the actin filament represents an unloaded velocity and does not directly give a measure of force production of the myosin (15). We do not know whether actin filaments traveling away from the center of the myosin filament can produce as much force as that which can be produced when the actin filaments are traveling toward the center. We note that vertebrate striated muscles that have undergone extensive contractions have reduced unloaded shortening velocities and force (16). During normal active contraction in vertebrate skeletal muscle the precise arrangement of the myosin and the actin filaments and the Z-line limit the extent to which the actin filament can cross the bare zone (1). In the cytoplasm of nonmuscle and some smooth muscle cells, actin filaments display a broad range of lengths and maintain very complex relation with myosin filaments (7). Our results suggest that any given orientation of the polar actin filaments can interact with any portion of the myosin filament and still contribute to force generation and movement.

REFERENCES AND NOTES

- H. E. Huxley, *Science* **164**, 1356 (1969).
- Y. Y. Toyoshima *et al.*, *Nature* **328**, 536 (1987).
- S. J. Kron and J. A. Spudich, *Proc. Natl. Acad. Sci. U.S.A.* **83**, 6272 (1986).
- Native thick filaments from the pink adductor muscle of *Mercinaria mercinaria* were prepared by a modification of the method of A. Yamada, N. Ishii, T. Shimmen, and K. J. Takahashi [*J. Muscle Res. Cell Motil.* **10**, 124 (1989)]. The preparation yielded myosin filaments of various lengths (mean = 9.5 ± 3.8 μm).
- B. Kachar, P. C. Bridgman, T. S. Reese, *J. Cell Biol.* **105**, 1267 (1987).
- Molluscan thick filaments are formed by polymerization of myosin around a core of paramyosin. [A. G. Szent-Györgyi, C. Cohen, J. Kendrick-Jones, *J. Mol. Biol.* **56**, 239 (1971)]. These filaments have been shown to be bipolar and are activated upon binding of calcium to the myosin molecules.
- S. J. Smith, *Science* **242**, 708 (1989); A. D. Bershadsky and J. M. Vasiliev, *Cytoskeleton* (Plenum, New York, 1988).
- D. A. Winklemann and S. Lowey, *J. Mol. Biol.* **188**, 595 (1986); R. Craig *et al.*, *ibid.* **140**, 35 (1980).
- M. Walker and J. Trinick, *ibid.* **192**, 661 (1986); *J. Muscle Res. Cell Motil.* **9**, 359 (1988).
- M. C. Reedy *et al.*, *Nature* **339**, 481 (1989).
- D. G. Stephenson, A. W. Stewart, G. J. Wilson, *J.*

- Physiol. (London)* **410**, 351 (1989).
- Y. Y. Toyoshima, C. Toyoshima, J. A. Spudich, *Nature* **341**, 154 (1989).
- W. F. Harrington, *Proc. Natl. Acad. Sci. U.S.A.* **76**, 5066 (1979).
- M. Stewart, A. D. McLachlan, C. R. Calladine, *Proc. R. Soc. London Ser. B* **229**, 381 (1987).
- A. Kishino and T. Yanagida, *Nature* **334**, 74 (1988).
- A. M. Gordon, A. F. Huxley, F. J. Julian, *J. Physiol. (London)* **184**, 170 (1966).
- For the *in vitro* motility assay native myosin filaments were diluted to a concentration of 30 to 50 $\mu\text{g/ml}$ and applied to a flow cell prepared according to Toyoshima *et al.* (12) except that nitrocellulose was not used to coat the cover slip. The flow cell was washed with a buffer containing bovine serum albumin (1 mg/ml), and motility was initiated by the

addition of 20 mM KCl, 20 mM MOPS (pH 7.2), 5 mM MgCl_2 , 1 mM adenosine triphosphate (ATP), 0.1 mM EGTA, 0.2 mM CaCl_2 , 1 mM dithiothreitol (DTT), 5 nM rhodamine phalloidin-labeled actin, 2.5 mg/ml glucose, 0.2 mg/ml glucose oxidase, and 0.02 mg/ml catalase at 25°C. The latter three components have been shown to retard photobleaching (15). The fluorescence images were recorded on optical memory disk with a SIT video camera (DAGE-MTI).

- We thank A. G. Szent-Györgyi for suggesting clam muscle, E. V. Harvey for technical assistance, M. Frey for help with the graphics, and P. Vibert, R. Levine, J. Fex, and R. S. Adelstein for helpful discussions.

2 March 1990; accepted 23 May 1990

Autophosphorylation of Protein Kinase C at Three Separated Regions of Its Primary Sequence

ANDREW J. FLINT, RUDOLPH D. PALADINI, DANIEL E. KOSHLAND, JR.*

The major autophosphorylation sites of the rat β II isozyme of protein kinase C were identified. The modified threonine and serine residues were found in the amino-terminal peptide, the carboxyl-terminal tail, and the hinge region between the regulatory lipid-binding domain and the catalytic kinase domain. Because this autophosphorylation follows an intrapeptide mechanism, extraordinary flexibility of the protein is necessary to phosphorylate the three regions. Comparison of the sequences surrounding the modified residues showed no obvious recognition motif nor any similarity to substrate phosphorylation sites, suggesting that proximity to the active site may be the primary criterion for their phosphorylation.

THE CALCIUM- AND PHOSPHOLIPID-dependent protein kinase C is a central mediator of signal transduction in the nervous system and other cell types (1). It phosphorylates substrates on serine or threonine residues in response to the lipophilic diacylglycerol (DAG) produced by phospholipase C (2). In addition to phosphorylating substrates, protein kinase C also phosphorylates itself (3–6). Autophosphorylation has been shown to alter the affinity of the protein for the tumor-promoting phorbol esters (4), to increase its sensitivity to calcium (4), and to increase its rate of H1 histone phosphorylation (5). Autophosphorylation has also been proposed to alter the association of protein kinase C with membranes (7) and to increase the enzyme's sensitivity to proteolytic down-regulation (8).

Autophosphorylation of protein kinase C follows an intrapeptide mechanism in which a single polypeptide chain phosphorylates itself (9). The evidence for this surprising finding is obtained with mixed micelles (10) that harbor a single protein molecule per

micelle. The rate of autophosphorylation is independent of protein concentration and is the same as the rate measured with lipid bilayers, a more physiological condition (9). This mechanism contrasts with that of the insulin receptor (11), the type II cyclic adenosine monophosphate (cAMP)-dependent protein kinase (12), the cyclic guanosine monophosphate (cGMP)-dependent protein kinase (13), and the calcium calmodulin-dependent protein kinase (14); these are multisubunit kinases and apparently undergo interpeptide autophosphorylation. Surprisingly, both the catalytic kinase domain and the regulatory lipid-binding domain of protein kinase C are phosphorylated in this reaction (4, 5, 9). These observations raise important questions about the understanding of protein structure and the regulation of this critical enzyme, and therefore, we have identified the modified residues in the primary sequence.

The gene encoding a rat β isozyme of protein kinase C (PKC β II) was cloned into a baculovirus expression vector and the protein was purified from Sf9 insect cells infected with the recombinant baculovirus (Fig. 1). The purified PKC β II was identical to the enzyme purified from rat brains by all criteria examined. The recombinant protein comigrated on an SDS-polyacrylamide gel

Department of Molecular and Cellular Biology, Division of Biochemistry and Molecular Biology, University of California, Berkeley, Berkeley, CA 94720.

*To whom correspondence should be addressed.

with the 80-kilodalton protein kinase C from rat brain, unlike the inactive protein synthesized in *Escherichia coli* (15) or the in vitro translation product analyzed by Parker *et al.* (16), which both show increased electrophoretic mobilities. The NH₂-terminus of the insect cell-expressed enzyme was blocked to automated Edman degradation, as are the rat and bovine brain enzymes (16, 17). Both autophosphorylation and phosphorylation of the H1 histone substrate by this enzyme are dependent upon calcium and the lipid activators, phosphatidylserine and DAG. The autophosphorylated tryptic peptides of the β II isozyme were identical to those obtained from a purified fraction of rat brain enzyme that was separated on hydroxylapatite (18).

Autophosphorylation of the recombinant β II enzyme, under conditions in which the ratio of micelles to kinase assures intrapeptide modification (9), maximally incorporated approximately 1.5 mol of phosphate per mole of kinase. The phosphorylated enzyme was digested with trypsin and the resulting peptides were separated by reversed-phase high-performance liquid chromatography (HPLC) (Fig. 2). Radioactive peak fractions were further purified on a narrow bore HPLC column at a different pH, where individual peaks of ultraviolet absorbing material were collected. The radioactive phosphopeptides were sequenced by automated Edman degradation and analyzed for their phosphoamino acid content. Identical results were obtained with two different preparations of recombinant PKC β II. The sequences obtained and the location of the modified amino acids are shown in the context of the primary structure of protein kinase C (Fig. 3). Identical results were obtained when autophosphorylation was performed with sonicated dispersions of phosphatidylserine and DAG instead of mixed micelles. When the reaction was car-

ried out for shorter times or was performed in the absence of calcium and phospholipid, the same phosphopeptides were detected but each was less extensively phosphorylated.

Phosphorylated threonine residues were readily identified. Instead of finding a phenylthiohydantoin (PTH)-threonine derivative, as expected from the sequence of the cDNA clone (17), two sets of characteristic breakdown products were obtained (19). They were observed in place of all predicted threonines except Thr³²¹, which was not phosphorylated. The symmetrical shape of each peptide collected from the second HPLC column and the absence of PTH-threonine at the phosphorylated position indicated that the phosphopeptides had been purified away from their nonphosphorylated progenitors. Phosphoamino acid analyses indicated that only the NH₂-terminal peptide contained phosphoserine. The modified residue was determined to be Ser¹⁶ as digestion of the tryptic peptide with V8 protease, which cleaves after glutamate, yielded a single phosphopeptide that contained both phosphoserine and phosphothreonine.

The COOH-terminal peptide typically contained the least [³²P]phosphate, but the recovery of its PTH-amino acids was approximately four times as great as expected, suggesting that Thr⁶³⁴ and Thr⁶⁴¹ were already partially phosphorylated. For the three other phosphopeptides, the number of moles of [³²P]phosphate was commensurate with the peak heights obtained on the PTH-amino acid analyzer. That the protein kinase C isolated from the insect cells may already be partially phosphorylated is consistent with the measurement of phosphate in the enzyme purified from rat brains (20) and with the immunoprecipitation of the radioactive protein from ³²P-labeled tissue culture cells (6).

Examination of the sequences around the phosphorylation sites revealed no obvious similarities that might be construed as a recognition motif. Neither did these peptide sequences show significant similarity to protein kinase C substrate phosphorylation sites, nor to synthetic peptide substrates in which the most readily phosphorylated serines or threonines are generally flanked by basic residues (21). However, these autophosphorylation events did exhibit selectivity, as Thr³¹⁴ and Thr³²⁴ were modified, while Thr³²¹ and Ser³²⁶ were not. The proximity of these sequences to the active site and conformational constraints on the peptide chain probably target particular residues for modification.

The location of these phosphorylated peptides in three widely separated regions of the primary sequence of protein kinase C was unusual, particularly in light of the intrapeptide mechanism of the autophosphorylation. The four peptides were found in three distinct, poorly conserved regions of the primary sequence: the NH₂-terminal peptide, the COOH-terminal tail, and the hinge region between the lipid-binding regulatory domain and the catalytic kinase domain (Fig. 3). The autophosphorylation

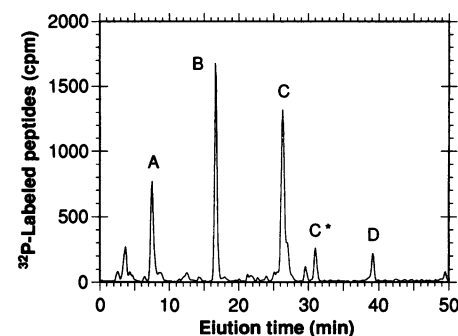
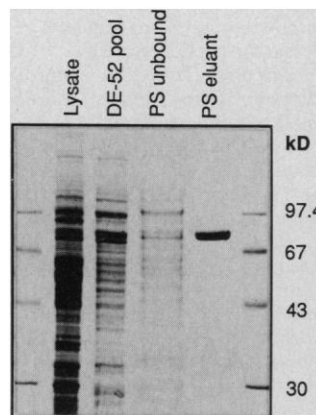


Fig. 2. Separation of autophosphorylated tryptic peptides of protein kinase C by reversed-phase HPLC. Radioactivity eluting from the HPLC column is displayed against elution time. Peaks of phosphopeptides that were sequenced are labeled (A, B, C, C*, D); C* was an incomplete digestion product of C. Protein kinase C was autophosphorylated and subjected to SDS-PAGE (9). The gel was stained with Coomassie, destained with acetic acid (10%), and dried onto filter paper. The slice of gel containing protein kinase C was rehydrated in 0.1 M NH₄HCO₃, macerated, and digested overnight at 37°C with 20 μ g of trypsin (TPCK-treated, Worthington). Soluble radioactivity (>85% of total counts per minute) in peptides was separated on a reversed-phase HPLC column (LC318, 4.6 mm by 25 cm, Supelco) in 20 mM sodium phosphate, pH 2.5. Phosphopeptides were eluted at 1 ml/min with a gradient from 2.5 to 30% acetonitrile between 5 and 45 min. Radioactivity was detected with an on-line scintillation detector (Radiomatic Instruments). These HPLC peaks appeared to represent all the major autophosphorylated peptides, as they accounted for all the phosphopeptides in a two-dimensional peptide map of a complete tryptic digest of the autophosphorylated protein.

Fig. 1. Purification of protein kinase C from insect cells infected with recombinant baculovirus. Proteins from the indicated stages of the purification were separated by SDS-polyacrylamide gel electrophoresis (SDS-PAGE) and stained with Coomassie brilliant blue. The recombinant baculovirus was obtained as described (25), except Lipofectin Reagent (BRL) was used for cotransfections. A Fnu DII fragment containing the entire coding region for the rat PKC β II gene was cloned into a filled-in Bam HI site, creating a Bam HI site located six nucleotides from the predicted initiator methionine. This Bam HI fragment was inserted into the baculovirus transfer vector, pAc373. Three or four days after infection of Sf9 cells with the recombinant baculovirus, protein kinase C was purified to a specific activity of ~ 1000 nmol min⁻¹ mg⁻¹. The only critical modification of this procedure (26) was that the DEAE column eluate was diluted 4:1 instead of 1:1 with the calcium-containing buffer before application to the phosphatidylserine (PS) affinity matrix. Protein kinase C-containing fractions were further purified on a Mono Q HR 5/5 column (Pharmacia-LKB) to remove a persistent phosphatase activity, which manifested itself during trypsin digestion of the autophosphorylated enzyme.



sites in the NH₂-terminal portion and in the hinge region are unique to the β isozymes, thus predicting that the pattern of autophosphorylation peptides will be different for the α or γ isozyme. The sequence surrounding the COOH-terminal sites is more conserved among the isozymes, despite being the only difference between the βI and βII proteins. The two autophosphorylated threonines in this region are found in all four α, βI, βII, and γ subspecies implying a common function for their phosphorylation.

Autophosphorylation of the NH₂-terminal peptide of PKC βII provides strong evidence for the proposed inhibitory role of the adjacent sequence. Many regulated kinases are suspected of being controlled by a pseudosubstrate inhibitor sequence whose purpose is to diminish the activity of the enzyme prior to stimulation (22). When an activating ligand (DAG, cAMP, cGMP, or calcium-calmodulin) is bound, this inhibitory peptide is postulated to be dislodged from the active site to allow substrate binding. The region between amino acids 19 and 31 has been proposed to serve this inhibitory function in protein kinase C (23). The autophosphorylation of Ser¹⁶ and Thr¹⁷ indicates that the segment of the protein con-

taining the inhibitory sequence is accessible to the active site.

The phosphorylation of multiple residues in a single polypeptide chain catalyzed by that same polypeptide requires significant protein flexibility. Each modified region of the protein must lie sufficiently close to the active site in the folded structure so that each serine or threonine to be modified can make contact with the essential catalytic amino acid side chains. One possible arrangement of the peptide chain shows the autophosphorylated residues in proximity to the adenosine triphosphate (ATP) binding cleft (Fig. 4). Even so, considerable protein flexibility would still be required because all potential phosphorylation sites cannot simultaneously occupy the active site. Because only one or two phosphates were incorporated into each protein kinase C polypeptide, all potential sites were not modified in any one protein molecule. Phosphorylation of one residue might hinder the subsequent phosphorylation of the other sites.

Phosphorylation at multiple sites could be a mechanism to produce several protein kinases with slightly altered specificities. Autophosphorylation is known to affect the

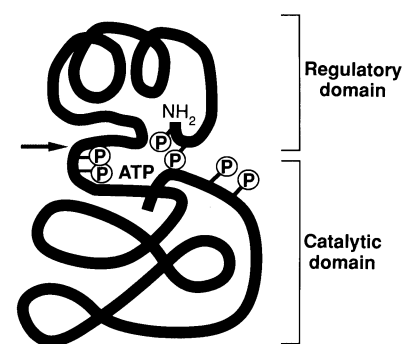


Fig. 4. Illustration of protein kinase C with the six autophosphorylation sites located close to the catalytic site. Each phosphorylation site is marked, although an individual molecule of protein kinase C would not have every site modified. An arrow marks the trypsin-sensitive cleavage site which separates the two domains. It is shown on the NH₂-terminal side of the phosphorylation sites in the hinge region because these phosphopeptides were found in the catalytic domain when the tryptic peptides obtained from each isolated domain were analyzed by HPLC.

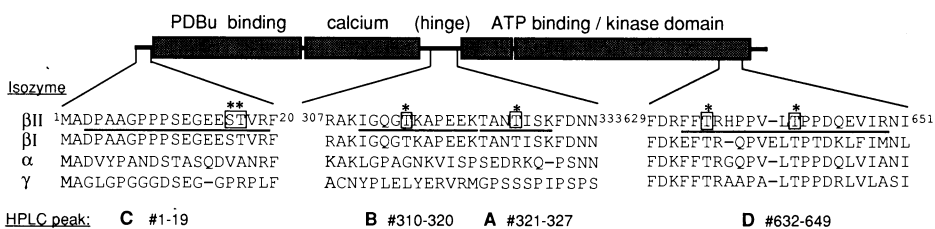


Fig. 3. Linear representation of the primary sequence of protein kinase C showing the location of the autophosphorylation sites in PKC βII. The sequences obtained from the tryptic phosphopeptides are underlined and the autophosphorylation sites are boxed and marked with an asterisk (*). The corresponding regions and flanking sequences of the rat α, βI, and γ isozymes are aligned for comparison (27). The HPLC peak corresponding to each underlined peptide is listed below the sequence with its amino acid residue numbers. The numbering of the amino acids (also shown in superscripts) is taken from the sequence predicted from cDNA cloning (17). The hatched regions represent amino acid sequences that are conserved among the α, β, and γ isozymes. The percent identities are 81% in the cysteine-rich phorbol ester (PDBu) binding region, 67% in the region conferring calcium sensitivity to PDBu binding (28), and 72% across the ATP-binding and kinase domain (29). The lines connecting conserved domains show no significant similarities. The βI and βII isozymes differ only in their final 50 amino acids. To obtain the peptide sequences, PKC βII (1 nmole) was autophosphorylated for 20 min in the presence of mixed micelles (0.1% Triton X-100 w/v, final concentration) containing phosphatidylserine:diacylglycerol:Triton X-100, 10:5:85 (mol %), 1.5 mM CaCl₂, and 100 μM [³²P]ATP (1000 cpm/pmol) (9). The autophosphorylated enzyme was separated from unincorporated ATP on a column (1 by 15 cm) of Sephadex G-50 fine (Pharmacia-LKB) equilibrated in 100 mM tris-HCl, pH 8.0. Fractions containing protein kinase C were digested overnight at 37°C with TPCK-trypsin (1/25 by weight). Tryptic peptides were separated on a reversed-phase HPLC column (LC318, 4.6 mm by 25 cm, Supelco) in 20 mM triethylamine phosphate, pH 6.5 at 1 ml/min with a gradient from 2.5 to 30% acetonitrile between 5 and 45 min. Peaks of radioactivity were individually applied to a Vydac C18 column (2.1 mm by 25 cm) on an Applied Biosystems 130A HPLC. Peptides were injected and the column washed for 10 min at 200 μl/min with 20 mM sodium phosphate, pH 2.5. A linear 80-min gradient to 30% acetonitrile was delivered at 100 μl/min. Fractions were collected manually following the absorbance of peptides at 214 nm. Radioactive peptides were sequenced by automated Edman degradation on an Applied Biosystems 477A instrument with a 120A analyzer. Peptide C was further digested overnight at room temperature with 2 μg of Asp N protease (Boehringer Mannheim) to remove the blocked NH₂-terminus. The product was repurified on the narrow bore C18 column before sequencing. Phosphoamino acids were obtained by partial acid hydrolysis of a sample of the purified peptide and were resolved by two-dimensional thin-layer electrophoresis (30).

binding affinity for phorbol esters (4), the sensitivity to calcium activation (4), and the phosphorylation rates of H1 histone (5). Phosphorylation of residues in the hinge region, close to the site of cleavage by the calcium-dependent protease, calpain (24), may alter the susceptibility of PKC βII to proteolysis, thus affecting the down-regulation of the enzyme. A catalytically inactive, ATP binding site mutant of PKC α is substantially resistant to down-regulation in fibroblasts (8). Finally, phosphorylation of the threonine residues in the COOH-terminal region of the catalytic domain is reminiscent of the similarly located autophosphorylation site of pp60^{c-src} (Tyr⁵²⁷) and other tyrosine kinases, which may function in the regulation of their kinase activities.

Thus four peptides containing six major sites of intrapeptide autophosphorylation of protein kinase C have been identified. Identification of an enzyme that modifies itself in three distinct regions of the primary sequence has intriguing implications for both protein flexibility and the control of biological function.

REFERENCES AND NOTES

1. Y. Nishizuka, *Science* **233**, 305 (1986); U. Kikkawa, A. Kishimoto, Y. Nishizuka, *Annu. Rev. Biochem.* **58**, 31 (1989).
2. M. J. Berridge and R. F. Irvine, *Nature* **312**, 315 (1984).
3. U. Kikkawa *et al.*, *J. Biol. Chem.* **257**, 3341 (1982).
4. K. P. Huang *et al.*, *ibid.* **261**, 2134 (1986).
5. D. Mochly-Rosen and D. E. Koshland, Jr., *ibid.* **262**, 2291 (1987).
6. J. R. Woodgett and T. Hunter, *Mol. Cell. Biol.* **7**, 85 (1987); F. E. Mitchell, R. M. Marais, P. J. Parker, *Biochem. J.* **261**, 131 (1989).
7. M. Wolf, P. Cuatrecasas, N. Sahyoun, *J. Biol. Chem.* **260**, 15718 (1985).
8. S. Ohno *et al.*, *ibid.* **265**, 6296 (1990).

9. A. C. Newton and D. E. Koshland, Jr., *ibid.* **262**, 10185 (1987).
10. Y. A. Hannun *et al.*, *ibid.* **260**, 39 (1985).
11. L. Petruzzelli, R. Herrera, O. M. Rosen, *Proc. Natl. Acad. Sci. U.S.A.* **81**, 3327 (1984); M. F. White, H.-U. Haring, M. Kasuga, C. R. Kahn, *J. Biol. Chem.* **259**, 255 (1984); M. A. Shia, J. B. Rubin, P. F. Pilch, *ibid.* **258**, 14450 (1983).
12. R. Rangel-Aldao and O. M. Rosen, *J. Biol. Chem.* **251**, 7526 (1976).
13. T. M. Lincoln, D. A. Flockhart, J. D. Corbin, *ibid.* **253**, 6002 (1978).
14. J. Kuret and H. Schulman, *ibid.* **260**, 6427 (1985).
15. A unique Nde I site was created at the initiator ATG of the PKC β II gene by site-directed mutagenesis. An Nde I-Bam HI fragment was cloned into pAR3040 to optimally align the gene behind a strong T7 phage promoter and Shine-Dalgarno sequence. Transformants of BL21 containing the resulting plasmid were examined for protein kinase C activity after induction with isopropyl- β -D-galactopyranoside.
16. P. J. Parker *et al.*, *Science* **233**, 853 (1986).
17. J. L. Knopf *et al.*, *Cell* **46**, 491 (1986).
18. K. P. Huang, H. Nakabayashi, F. L. Huang, *Proc. Natl. Acad. Sci. U.S.A.* **83**, 8535 (1986).
19. N. Dedner, H. E. Meyer, C. Ashton, G. F. Wildner, *FEBS Lett.* **236**, 77 (1988).
20. J. R. Woodgett and T. Hunter, *J. Biol. Chem.* **262**, 4836 (1987).
21. C. House, R. E. H. Wettenhall, B. E. Kemp, *ibid.*, p. 772.
22. G. Hardie, *Nature* **335**, 592 (1988).
23. C. House and B. E. Kemp, *Science* **238**, 1726 (1987).
24. A. Kishimoto *et al.*, *J. Biol. Chem.* **264**, 4088 (1989).
25. M. D. Summers and G. E. Smith, *A Manual of Methods of Baculovirus Vectors and Insect Cell Culture Procedures* (Texas Agriculture Experiment Station, College Station, TX, 1987).
26. T. Uchida and C. R. Filburn, *J. Biol. Chem.* **259**, 12311 (1984).
27. U. Kikkawa *et al.*, *FEBS Lett.* **223**, 212 (1987).
28. Y. Ono *et al.*, *Proc. Natl. Acad. Sci. U.S.A.* **86**, 4868 (1989).
29. L. Coussens *et al.*, *Science* **233**, 859 (1986).
30. J. A. Cooper, B. M. Sefton, T. Hunter, *Methods Enzymol.* **99**, 387 (1983).
31. We thank the Howard Hughes Medical Institute and A. Admon for his expertise in peptide sequencing; J. Knopf for the full-length rat PKCII cDNA; M. Summers for the baculovirus starter kit; and H. Biemann for recommending the phosphatidylserine affinity matrix. Supported by NIH grant DK09765 and NSF grant 840200.

12 March 1990; accepted 25 May 1990

Four-Dimensional Heteronuclear Triple-Resonance NMR Spectroscopy of Interleukin-1 β in Solution

LEWIS E. KAY, G. MARIUS CLORE, AD BAX, ANGELA M. GRONENBORN

A method is presented that dramatically improves the resolution of protein nuclear magnetic resonance (NMR) spectra by increasing their dimensionality to four. The power of this technique is demonstrated by the application of four-dimensional carbon-13–nitrogen-15 (^{13}C - ^{15}N)–edited nuclear Overhauser effect (NOE) spectroscopy to interleukin-1 β , a protein of 153 residues. The NOEs between NH and aliphatic protons are first spread out into a third dimension by the ^{15}N chemical shift of the amide ^{15}N atom and subsequently into a fourth dimension by the ^{13}C chemical shift of the directly bonded ^{13}C atoms. By this means ambiguities in the assignment of NOEs between NH and aliphatic protons that are still present in the three-dimensional ^{15}N -edited NOE spectrum due to extensive chemical shift overlap and degeneracy of aliphatic resonances are completely removed. Consequently, many more approximate interproton distance restraints can be obtained from the NOE data than was heretofore possible, thereby expanding the horizons of three-dimensional structure determination by NMR to larger proteins.

OVER THE LAST FEW YEARS IT HAS been shown that two-dimensional (2D) NMR spectroscopy (1) can be used to determine the solution structures of small proteins (≤ 100 residues) at a resolution comparable to that attainable by x-ray crystallography (2–4). The initial stage in an NMR structure determination involves spectral assignment by means of experiments that demonstrate through-bond and through-space correlations (5). The principal source of geometric information resides in short ($< 5 \text{ \AA}$) approximate interproton

distance restraints derived from NOE experiments, and the accuracy and precision of an NMR structure determination depends critically on the number of restraints that can be extracted from the data (3, 4). The application of 2D NMR methods to larger proteins has been impeded by two factors. First, the increase in the number of resonances leads to severe chemical shift overlap and degeneracy, rendering the assignment of through-bond interactions or through-space interactions or both increasingly difficult. Second, the increase in molecular weight results in larger linewidths so that the sensitivity of through-bond correlation experiments based on small ($< 12 \text{ Hz}$) homonuclear couplings is much reduced.

Many of the uncertainties present in 2D NMR spectra can be resolved by spreading out the 2D spectra into a third dimension (6), and NMR techniques based on large heteronuclear couplings should permit applications to larger proteins (7). To this end a number of three-dimensional (3D) heteronuclear NMR experiments that rely on large resolved heteronuclear couplings have been developed (8–13) and have been shown to be highly efficient for spectral assignment of proteins labeled with ^{15}N or ^{13}C or both up to a molecular weight of about 20 kD (14). Despite this added resolution, ambiguities still remain in the interpretation of 3D heteronuclear NMR spectra of larger proteins, so that an additional increase in resolution afforded by raising the dimensionality still further is desirable. In this paper we report a four-dimensional (4D) NMR experiment and demonstrate its applicability to uniformly labeled ^{15}N - ^{13}C interleukin-1 β (IL-1 β), a 17.4-kD protein of 153 residues, that plays a central role in the immune and inflammatory responses (15).

All 2D NMR experiments comprise four distinct steps, namely, preparation, evolution, mixing, and detection (16). A 4D NMR experiment is easily conceived by combining three 2D NMR experiments, leaving out the detection period of the first, the preparation and detection periods of the second, and the preparation period of the third. The 4D experiment we have chosen to perform is one in which NOEs between NH protons and aliphatic protons are spread out by the chemical shifts of the directly bonded ^{15}N and ^{13}C atoms, respectively. The rationale behind this experiment lies in resolving extensive ambiguities still present in a 3D ^{15}N -edited NOESY experiment (3D ^1H - ^{15}N NOESY-HMQC) in which NOEs between NH protons and aliphatic protons are spread into the third dimension by the chemical shift of the directly bonded ^{15}N atoms (8, 9). Although this 3D experiment effectively removes, in all but a very few cases, chemical shift degeneracy associated with the NH protons, it leaves the ambiguities associated with severe overlap of aliphatic resonances unaffected. Thus, even if a cross peak connecting an aliphatic and amide proton is well resolved in the 3D spectrum, it is frequently not possible, with the exception of cases involving the CaH resonances, to identify conclusively the aliphatic proton involved on the basis of its ^1H chemical shift.

The progression and relation between ^{15}N - ^{13}C -heteronuclear-edited 2D, 3D, and 4D NOESY experiments is illustrated schematically in Fig. 1. In the 2D spectrum, NOEs between NH protons (F_2 dimension) and aliphatic protons (F_1 dimension) are

Laboratory of Chemical Physics, National Institute of Diabetes and Digestive and Kidney Diseases, National Institutes of Health, Bethesda, MD 20892.